LANGMUIR

pubs.acs.org/Langmuir Article

New Method to Probe the Surface Properties of Polymer Thin Films by Two-Dimensional (2D) Inverse Gas Chromatography (iGC)

Whirang Cho, Lucas Q. Flagg, John R. Hoffman, Daniel Burnett, Anett Kondor, Douglas M. Fox, Christopher M. Stafford, and Jeremiah W. Woodcock*

Cite This: *Langmuir* 2024, 40, 14037−14044 Read Online

ACCESS | Metrics & More | Article Recommendations | Supporting Information

ABSTRACT: Polymer-based functional surface coatings are extensively used in advanced technologies, including optics, energy, and environmental applications. Surface thermodynamic properties profoundly impact the molecular interactions that control interfacial behaviors, such as adhesion and wettability, which in turn dictate coating processes and performance. Conventionally, contact angle measurements are used to assess the surface energy of polymer films and coatings, where the wettability of a surface is assessed using probe fluids (liquid drops). However, contact angle measurement oftentimes can be nontrivial due to the roughness or chemical heterogeneity of the solid surface, as well as the potential for the liquid drop to swell or even dissolve the material being measured. Alternatively, inverse gas chromatography (iGC) is a versatile technique to measure surface thermodynamics and Lewis acid−base properties while also providing environmental control such as temperature and humidity. Despite these benefits, the application of iGC has been limited to powders or fibers, while the direct measurement of supported thin films or coatings is still a nascent area of research. This creates a challenge when using iGC as a comprehensive platform for measuring the physicochemical properties of solid surfaces. Here, we demonstrate how to effectively use iGC to characterize the surface energy of supported polymer thin films by using a two-dimensional (2D) film holder and modifying operational controls, such as the concentration range of the injected gas probe molecules. This enables the precise control of surface coverage required for analyzing samples having minimal surface area, such as thin films. Poly(methyl methacrylate) (PMMA) was employed as a benchmark to determine suitable iGC parameters and to validate our approach on polymer thin films. The seminal work presented here expands the capability of state-of-the-art iGC to embrace supported thin films (2D iGC) that could either be smooth or display texture/roughness (patterned films) as well as coatings with heterogeneous chemical/structural composition.

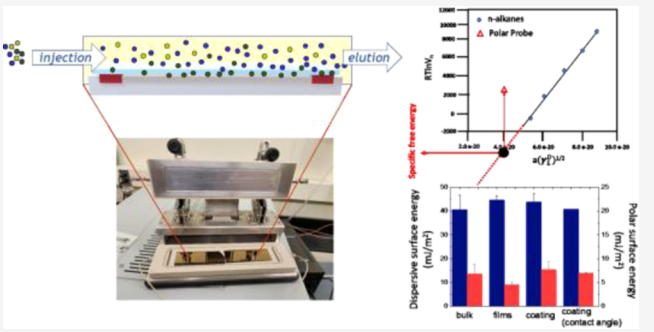

INTRODUCTION

Surface engineering truly epitomizes enabling technology. For example, coatings are often limited by surface requirements involving enhanced friction, wear, and corrosion resistance,[1,2] and engineering the surface of those coatings, either through chemistry or processing, can impart advanced properties and/or function for specific applications. Some examples of surface properties include wettability and surface energetics, which provide important metrics for interfacial behavior, physical stability, processability, and more. Recently, adhesion and stability of polymer thin films have demanded increasing attention due to opportunities in advanced electronics, packaging, wearable sensors, and solar cells.[3−7] The surface energy of a material is defined as the energy required to produce a unit area of a new surface; two main components, the dispersive and polar surface energy, contribute to the calculation of the total surface energy. Dispersive surface energy results from long-range intermolecular forces caused by the interactions between electronic dipoles and induced dipoles in neighboring molecules or atoms.[8] On the other hand, polar surface energy originates from specific interactions such as hydrogen bonding and Lewis acid−base interactions.[9] Both of these forces consequently control the nature of chemical interactions at the surface of a material, determining hydrophobicity, reactivity, and polarity.[10] Consequently, there exists a growing need to precisely measure the surface energy and surface energy heterogeneity of supported polymer thin films. Specifically, the measurement capability of coatings having a diverse range of surface topographies is indispensable to better understand advanced coatings in their native forms.

Received: April 15, 2024
Revised: June 8, 2024
Accepted: June 10, 2024
Published: June 25, 2024

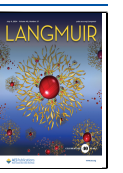

https://doi.org/10.1021/acs.langmuir.4c01400
Langmuir 2024, 40, 14037−14044

Typically, this information is obtained by the measurement of the three-phase contact angle (solid−liquid−vapor) of solvents on a flat surface composed of the material of interest. The contact angle method measures the wettability of a surface or interface with a liquid droplet to assess the surface energy of polymer thin films,[11] with the measurand being the angle the droplet makes at the three-phase boundary between the droplet and the surface. However, despite its accessibility, there are some pitfalls associated with the measurement. By definition, contact angle measurements only interrogate the average surface properties along the perimeter of the droplet, where the three-phase contact line exists and is challenged by surface heterogeneity. Moreover, the surface roughness and chemical heterogeneity of a solid surface oftentimes make it difficult to measure contact angle values.[12,13] As the telescope-goniometer method has an intrinsic drawback pertaining to the assignment of tangent lines on a flat drop contour, it suffers from errors when the contact angle is below 20°.[14,15] Furthermore, the contact angle can be misleading due to solvent purity, liquid sorption, or solid swelling by probe liquids.[16] Considering the high fidelity and nondestructive testing capabilities of inverse gas chromatography (iGC), the advancement of surface characteristics techniques encompassing different physical sample forms based on iGC is of great interest. This could complement contact angle measurements effectively when it comes to surfaces with topographic features and chemical heterogeneity.

iGC is often used to measure the thermodynamic properties of solids using isotherms under controlled humidity to assess surface energy and surface energy heterogeneity for a sample of interest.[17] This measurement has been mainly applied to particulate or fibrous materials, including polymer pellets or powders,[18,19] inorganic compounds and catalysts,[20,21] food substances,[22] carbon nanotubes,[23] wood composites,[24] and pharmaceuticals.[25] Essentially, iGC is a vapor sorption technique: gas probes of known cross-sectional area and thermodynamic properties are flowed into a column containing the samples of interest, and the elution time is recorded as the measurement output. This elution time can be regarded as the retention time of the probe molecules by the sample, t_R, and is governed by the magnitude of sample−probe interactions.[26] Conventional column-based iGC has been extensively used for measuring the surface properties of porous media and fibers, and it has been recently used to study the diffusion and permeability of gases through polymer coatings on glass beads.[27] Nevertheless, these methods are limited to powdered samples, while the measurement of 2D materials (i.e., thin films or coatings) is still nascent and being developed.[28,29] In this work, we examine the metrology of iGC as applied to the investigation of supported thin films, highlighting a different approach to obtain their thermodynamic properties. Poly(methyl methacrylate) (PMMA) is used as a model polymer to validate our approach, which encompasses different physical sample forms, ranging from bulk materials to thick films to thin films. The use of a clamshell-type sample holder in lieu of a column is introduced, which allows for the study of freestanding and substrate-supported thin films. The specific (acid−base) and total surface energies of PMMA in the different sample geometries were compared. Additionally, we demonstrate the ability to differentiate two films of poly(acrylic acid) (PAA) with different degrees of ionization at pH values of 2 and 7 through acid−base constants. Finally, we explore the ability of iGC to sense the surface energy heterogeneity (both chemical and roughness) of a poly(ethylene oxide) (PEO) thin film arising from its semicrystalline nature.

EXPERIMENTAL SECTION

General. Certain equipment, instruments, software, or materials are identified in this work in order to specify the experimental procedure adequately. Such identification is not intended to imply recommendation or endorsement of any product or service by NIST, nor is it intended to imply that the materials or equipment identified is necessarily the best available for the purpose.

Materials and Coating Preparation. Nonpolar probes (decane, nonane, octane, heptane, and hexane) and polar probes (dichloromethane (DCM), ethyl acetate (EA), acetonitrile, acetone, and ethanol) with HPLC purity were obtained from Sigma-Aldrich (St. Louis, MO). Poly(methyl methacrylate) (PMMA, M_w: 177k g mol^{-1}), poly(acrylic acid) (PAA, M_w: 50k g mol^{-1}), and polyethylene oxide (PEO, M_w: 20k g mol^{-1}) were purchased from Sigma-Aldrich and used without further purification. M_w is the mass average relative molecular mass of each polymer. PMMA thin films were prepared via spin coating from a 2% by mass fraction solution in toluene. PEO thin films were prepared via spin coating from a 5% by mass fraction solution in toluene. PAA thin films were prepared via spin coating from a 2% by mass fraction solution in water (deionized, resistivity 18.2 MΩ). The pK_a of PAA is around 4.5, at which point half of the carboxylic acid pendent groups are ionized to carboxylate. Below this pH, the protonated form of the carboxylic acid pendent groups dominates, and thus, the film should display less ionic character. Above pH 4.5, the deprotonated or carboxylate dominates the polymer pendent groups. Initial solutions of PAA were found to have a pH of around 2 and thus represent samples containing fewer charged moieties. A daughter solution was then adjusted to pH ≈ 7 using 1 mol/L sodium hydroxide (NaOH) to increase the degree of ionization of the carboxylic acid groups.

Substrate-supported polymer thin films were prepared by using silicon wafers as the support. Silicon wafers were cleaned by sequential solvent washing with toluene, ethanol, and water, followed by ultraviolet−visible ozone (UVO) treatment for 20 min. To ensure that the iGC probe gases interact only with the thin polymer film and not the rough, unpolished backside of the silicon wafer substrate, we treated the backside of the wafer with a perfluorinated chlorosilane (1*H*,1*H*,2*H*,2*H*-perfluorooctyldimethyl chlorosilane, 97%) to render it inert. This chemistry is similar to what is done to the surface of traditional glass iGC sample columns to render them inert, preventing unwanted interactions between the probe gases and the column surface. Here, we first spin coat a sacrificial film of polystyrene (2% by mass fraction solution in toluene, thickness ≈ 120 nm) onto the polished side of the silicon wafer and then deposit the fluorosilane onto the backside of the wafer via a vacuum-assisted vapor phase reaction in a desiccator. After 12 h of reaction, the wafers were removed from the desiccator and sequentially rinsed with toluene, ethanol, and water. This removed both the protective polystyrene coating and any unreacted fluorinated silane, leaving a monolayer of fluorinated silane on only the backside of the wafer. We referred to these backside fluorinated silicon wafers as "f-Si." At this point, the polymer of interest (PMMA, PAA, or PEO) was spin-coated onto the polished side of the f-Si wafers and kept under a vacuum until the samples were loaded into the iGC clamshell sample cell.

Polarization Modulated Infrared Reflection Absorption Spectroscopy (PM-IRRAS). PM-IRRAS is a surface-enhanced IR spectroscopy technique for studying thin films and monolayers on an IR reflective substrate. Here, PM-IRRAS was performed on a Nicolet 6700 Fourier transform infrared (FTIR) spectrometer equipped with an external tabletop optical mount (TOM box), which includes a photoelastic modulator (PEM) set at a modulation frequency of 50 kHz and a maximum throughput of 2500 cm^{-1}, a dry-air-purged sample compartment (J.A. Woollam HTC-100), a liquid nitrogen-cooled Mercury Cadmium Telluride-A (MCT-A) detector, and an externally synchronized sampling demodulator. The detector was mounted at 70° with respect to the surface normal to maximize the

https://doi.org/10.1021/acs.langmuir.4c01400
Langmuir 2024, 40, 14037−14044

signal-to-noise ratio.[30] For these measurements, the polymer films were cast on Au-coated silicon wafers (Platypus Technologies, 100 nm Au on silicon), and FTIR spectra were recorded at a resolution of 4 cm^{-1} with a spectral range of 1000−4000 cm^{-1}. The spectra are shown in Figure S3. For the PAA film cast at pH 2, the FTIR peak at $\upsilon \approx 1730$ cm^{-1} can be assigned to the carbonyl stretching (C═O) of the carboxylic acid groups (COOH) (see Figure S3b). For the PAA cast at pH 7, the asymmetric stretching band of carboxylate groups (COO^-) at $\upsilon \approx 1600$ cm^{-1} is observed, whereas the carbonyl stretching peak from COOH significantly decreases (see Figure S3c). The ratio of $[COO^-]/[COOH]$ is ≈ 8.6, indicating that most of the COOH groups were deprotonated into the COO^- form.

Contact Angle Measurements. The Owens, Wendt, Rabel, and Kaelble (OWRK) approach is one of the most commonly used models to calculate the surface energy of a solid using the geometric mean of solid−liquid surface tension

$$\sqrt{\gamma_{sv}^{d}\gamma_{lv}^{d}} - \sqrt{\gamma_{sv}^{p}\gamma_{lv}^{p}} = 0.5\gamma_{lv}(1 + \cos\theta_Y) \quad (1)$$

where γ_{sv}^{d} and γ_{lv}^{d} are the dispersive components, γ_{sv}^{p} and γ_{lv}^{p} are the polar components of the solid (s) and liquid (l) surface energies, respectively, and θ_Y is the measured Young's contact angle. Since there are two unknowns in eq 1 (γ_{sv}^{d} and γ_{sv}^{p}), one needs to use at a minimum two probe fluids of known dispersive and polar components to solve for the polar and dispersive components of the solid surface energy. Water and diiodomethane were used as probe fluids: the dispersive surface tension of diiodomethane is 50.8 mN/m (no polar component), while the dispersive and polar surface tensions of water are 21.8 and 51.0 mN/m, respectively.

The contact angle was measured by a sessile drop method on an FTA125 contact angle analyzer (First Ten Angstroms). PAA and PEO thin films were annealed in a vacuum oven at 110 and 40 °C, respectively, for 2 h prior to the measurements to remove residual water. 20 μL of water and diiodomethane were manually dispensed from a syringe on the surface of polymer thin films, and the droplet images were captured by using a charge-coupled device (CCD) camera. The captured images were then analyzed by profile analysis tensiometer (PAT) 2.0 software to determine the advancing contact angles based on a curve fitting of each droplet.

Inverse Gas Chromatography (iGC). Surface energies were measured on an Inverse Gas Chromatography-Surface Energy Analyzer (iGC-SEA), Surface Measurement Systems (SMS), and the data were analyzed using advanced SEA Analysis Software. A mole injection method allowed more precise control of the gas probe injection concentration and the resulting surface coverage. For column experiments, powder and drop-cast thick film samples were packed into silanized glass columns with an internal diameter (ID) of 4 mm and a length of 30 cm. For substrate-supported thin films, the samples were placed in a tabletop clamshell-type film cell module (see Figure S1). The clamshell was designed to clamp down on both sides of a large sheet or composite laminate using the sample surface pressing against a gasket to help create an airtight seal. We modified the clamshell design to accommodate the silicon wafer substrates: the samples were placed in the bottom of the clamshell, and a thin stainless steel plate (230 × 60 mm) was inserted above the samples to create an airtight seal against the gasket. The surface area was determined based on the support geometry (i.e., total area of the silicon wafers). The surface area of each cut wafer was 20 cm^2, and multiple wafers were loaded into the 2D clamshell holder. After assembly, a leak detector was used to verify a tight seal. A low flow rate (6 SCCM) was used for each probe molecule to enhance the dwell times on the supported films. The retention time of methane gas was adjusted to 10 min to provide sufficient dwell time for the inert gas, which is a requisite for accurately determining the dead time (t_0).

Methods/Theory of iGC. A series of nonpolar probes (n-alkanes) as well as polar probes (with known Lewis acid−base interaction parameters) were passed through a 2D film cell module, and their retention time was measured. The retention time is affected by the adsorption/desorption of the probe molecules on the surface of samples, which is detected by the flame ionization detector (FID). The retention volume is determined from the retention time according to the following equation

$$V_n = \frac{j}{m} \times F \times (t_R - t_0) \times \frac{T_c}{273.15} \quad (2)$$

where j is the James−Martin pressure correction factor rendering retention volume independent of pressure, m is the sample mass, F is the exit flow rate, t_R is the retention time for the gas probes, t_0 is the time required for the noninteracting, nonadsorbed methane gas to pass through the column (i.e., the dead time), and T_c is the temperature of the column.[9,31,32] The retention volume is then used to determine the dispersive surface energy using the Schultz approach.[33] The relationship between the retention volume and dispersive surface energy can be determined using the following equation

$$RT \ln V_n = 2N_{Av}(\gamma_S^D)^{1/2}\alpha(\gamma_L^D)^{1/2} + constant \quad (3)$$

where R is the gas constant, T is the absolute temperature, V_n is the retention volume, N_{Av} is Avogadro's number, and α is the cross-sectional area of the nonpolar n-alkane molecule. The dispersive surface energy is calculated from the slope of the plot of $RT \ln V_n$ versus $(\gamma_L^D)^{1/2}$ of n-alkanes by injecting exceedingly small amounts of gas probe molecules (i.e., infinite dilution) into a column packed with the sample of interest. In this infinite dilution region, the retention time of the probes is independent of injection volume; therefore, a linear isotherm is obtained. The polar surface energy consists of Lewis acid (γ_S^+) and Lewis base (γ_S^-) parameters. Inclusion of polar probe gases that are Lewis acid or base in character allows us to access the specific free energy. Therefore, when $RT \ln V_n$ of polar probes is plotted against $(\gamma_L^D)^{1/2}$, the data are located above the alkane straight line.[31,34] (see Figure S2). The distance between those data points and the alkane line is associated with polar surface energy that accounts for specific interactions, including hydrogen bonding and short-range interactions such as Lewis acid−base reactions. For the analysis, the Van Oss, Chaduary, and Good approach[35] was applied to determine the specific surface energy according to the following equation

$$\Delta G^{SP} = 2N_{Av}\alpha(\sqrt{\gamma_L^+\gamma_S^-} + \sqrt{\gamma_L^-\gamma_S^+}) \quad (4)$$

where ΔG^{SP} is the specific component of the surface energy (mJ/mol), and γ_L^+ and γ_L^- (mJ/m^2) are the electron-acceptor (acid) and electron-donor (base) parameters of the monopolar basic probe, ethyl acetate (EA), and monopolar acidic probe, dichloromethane (DM), respectively. Using $\gamma_{DM}^+ = 5.20$ mJ/m^2 for dichloromethane and $\gamma_{EA}^- = 19.20$ mJ/m^2 for ethyl acetate, γ_S^+ and γ_S^- were determined, whose geometric mean is related to the specific surface energy.

$$\gamma_S^{SP} = 2\sqrt{\gamma_S^+\gamma_S^-} \quad (5)$$

The total surface energy of the sample of interest is defined as the sum of the dispersive and polar components.

$$\gamma_s^T = \gamma_s^D + \gamma_S^{SP} \quad (6)$$

To determine the surface energy heterogeneity, the adsorbed amount (n) and the resulting adsorption isotherm are obtained by integrating the net retention volume (V_N) as a function of equilibrium partial pressure (P). P can be estimated from the shape of the chromatogram according to the following equation

$$P = \frac{h_c}{F_c \times A_c} V_{Loop} \frac{273.15}{T_{Loop}} P_{inj} \quad (7)$$

where h_c is the chromatogram peak height, A_c is the chromatogram peak area, V_{Loop} is the injection loop volume, T_{Loop} is the injection loop temperature, and P_{inj} is the partial pressure of each solute. The actual fractional surface coverage is the number of moles injected (n) divided by the number of moles required to cover a theoretical monolayer surface coverage (n_m)

https://doi.org/10.1021/acs.langmuir.4c01400
Langmuir 2024, 40, 14037−14044

$$n_m = \frac{(SSA) \times m}{(Xsect) \times N_{Av}} \quad (8)$$

where *SSA* is the specific surface area (m^2/g), *m* is the sample mass (g), *Xsect* is the cross-sectional area of the probe molecule, and N_{Av} is Avogadro's number. n/n_m values range from 0 (i.e., infinite dilution) to 1.0 (i.e., monolayer coverage).

RESULTS AND DISCUSSION

The detection ranges of a conventional flame ionization detector (FID) used by iGC are highly sensitive, which is typically 0.1 to 1 × 10^5 ppm and well within the range required. However, its high reliance on the available surface area of the sample (≈ 0.5 m^2) poses restrictions to applying iGC to 2D polymer thin films. Standard practice in iGC is to inject a chosen concentration of probe molecules relative to a target surface coverage (n/n_m) of the sample.[31,32,34] The target surface coverage is determined by using the specific surface area as an input and is limited by the injection volume. Based on the specific surface area, the instrument will attempt to inject a partial pressure of probe gas that will interact with a target percentage of the available surface. This is normally not an issue in the conventional column configuration where decigram quantities of the sample are loaded into a column for measurement, and the sample mass can readily be adjusted.[31] For a 2D sample geometry, the specific surface area of the sample to be measured is markedly smaller and somewhat fixed. This was found to be problematic for obtaining small enough probe gas concentrations needed for 2D samples. As a result, modifications to the injection method and carrier gas flow rate were necessary. Using standard measurement methods, the actual surface coverage (n/n_m) values for the polymer thin-film samples tend to be higher than 1, possibly due to multiple-layer adsorption on the relatively small sample surface area compared to the powder or fiber samples commonly used with fractional surface coverage methods. Directly controlling the molar quantity of the injected probe gas enabled the precise control of the gas probe injection partial pressure. This can lead to fractional surface coverages usually in the range of n/n_m < 0.2 that are requisite for calculating the surface energies of 2D thin films and coatings.

PMMA is a well-studied polymer with documented thermodynamic properties and thus was selected as a model polymer. Conventional column measurements of PMMA powder and drop-cast thick films of PMMA were examined as a benchmark. These results were then compared to thin films on passivated silicon substrates by using the clamshell sample holder along with contact angle measurements to validate the 2D iGC methodology. All measurements were performed under ambient temperature and zero relative humidity, controlled by the carrier gas. The polar component of the surface energy was deconvolved into acid−base contributions by using a monopolar Lewis acid probe (dichloromethane) and a monopolar Lewis base probe (ethyl acetate). The retention time of each gas probe was converted to nonpolar (dispersive) and polar (acid−base) surface energies by applying Schultz[33] and Van Oss, Chaduary, and Good approaches,[35] respectively. Here, the surface energy for PMMA in these different physical forms was determined at identical injection concentrations of probe molecules ($n \approx 1E^{-05}$).

Similar surface energy values were found for the different forms of PMMA using iGC, as shown in Figure S4. The three different sample geometries of PMMA yielded similar results, which, although promising, should be compared to a complementary measurement such as contact angle. In this study, the Owens, Wendt, Rabel, and Kaelble (OWRK) model[9] was used to analyze surface energies based on contact angles. Table 1 summarizes the surface properties of PMMA in different sample forms, which reveals that the magnitude of dispersive surface energies obtained from iGC analysis is reasonably comparable to that obtained by contact angle measurement. These surface energy values obtained from iGC measurement are also reflective of averaged dispersive (37.2 ± 5.2 mJ/m^2) and polar (6.2 ± 4.0 mJ/m^2) components that are calculated by using previously examined values.[36,37] The polar component obtained from the OWRK model is influenced by hydrogen bonding and Coulomb interactions between dipoles (dipole−dipole and dipole-induced dipole) based on the probe fluids used. However, this model cannot account for all of the nondispersive interactions.[38] Furthermore, it is known that the surface energy calculated by most models is dependent on the selected probe fluids, which can be attributed to the slightly different specific energy components between iGC analysis and contact angle measurements, although the differences are admittedly small.

Table 1. Average Values of the Dispersive and Polar Components of the Surface Energies of Poly(methyl methacrylate) (PMMA, M_w: 177k g mol^{-1}) in Different Forms (Surface Energy Represents the Average and the Standard Deviation of Each Measured Data Point, n = 3)

samples	γ^D (mJ/m^2)	γ^P (mJ/m^2)	K_b/K_a
PMMA powder	40.6 ± 6.1	6.8 ± 2.0	9.7
PMMA bulk films	44.6 ± 1.9	4.6. ± 0.6	10.4
PMMA coating	43.8 ± 3.4	7.7 ± 1.7	11.1
*PMMA thin film	40.8 ± 0.1	7.0 ± 0.1	N/A

*These surface energies were calculated from the contact angle measurements of water and diiodomethane.

The Lewis acid parameter, K_a, and Lewis base parameter, K_b, indicating the propensity of the surface for either electrophilic or nucleophilic interactions, respectively, can be calculated using[39]

$$-H_{ads} = K_a \times DN + K_b \times AN \quad (9)$$

where H_{ads} is the enthalpy of adsorption, and *DN* and *AN* are Gutmann's electron pair donor and acceptor numbers of polar probe molecules, respectively. The absolute determination of H_{ads} is laborious, as it requires the measurements for every probe at least three different temperatures. As H_{ads} is proportional to the free Gibbs energy of adsorption, Gutmann developed a simplified approach by using ΔG^{SP} according to the following equation[19,40,41]

$$\Delta G^{SP} \approx K_a \times DN + K_b \times AN \quad (10)$$

where K_a and K_b can be obtained from the slope and intercept of the linear plot when plotting $\Delta G^{SP}/AN$ versus DN/AN, respectively. Generally, a reliable assessment of K_a and K_b depends on the linear correlation coefficient of $\Delta G^{SP}/AN$ versus DN/AN, which often leads to errors.[42] In lieu of discrete values, Table 1 shows the ratio of Lewis basicity to acidity (K_b/K_a), which represents the overall characteristic of a surface in terms of electron deficiency.[43] The data indicate that the surface of PMMA contains more Lewis basic sites, possibly

https://doi.org/10.1021/acs.langmuir.4c01400
Langmuir 2024, 40, 14037−14044

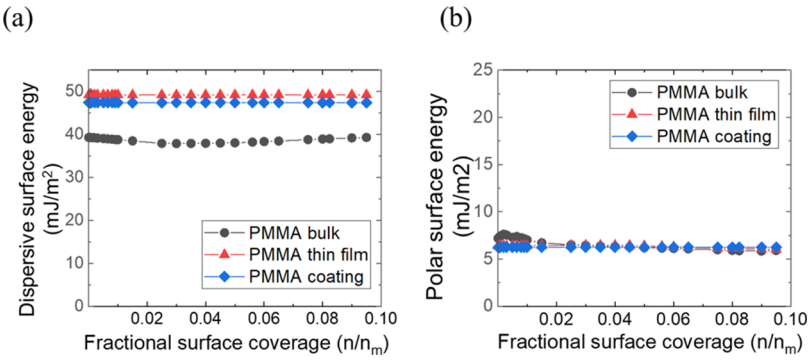

Figure 1. (a) Dispersive and (b) polar (acid−base) surface energy profiles of poly(methyl methacrylate) (PMMA, M_w: 177k g mol^{-1}) obtained from iGC analysis.

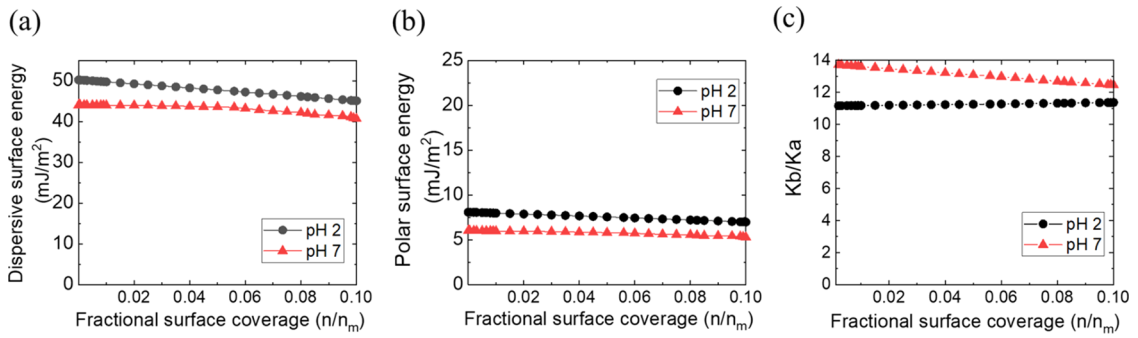

Figure 2. (a) Dispersive and (b) polar (acid−base) surface energy profiles of poly(acrylic acid) (PAA) coatings cast from aqueous solution at pH 2 and pH 7. (c) Lewis base parameter/acid parameter ratio (K_b/K_a) profile of PAA coatings cast from pH 2 and 7 solutions as a function of surface coverage (n/n_m).

due to the Lewis base nature of oxygen and the ester groups on the backbone, which is consistent with previous studies.[42,44]

iGC can also be effectively used to measure the surface energy and chemical heterogeneity of the sample as a function of surface coverage (n/n_m). Figure 1 shows the profiles of dispersive and polar (acid−base) surface energy for PMMA in different physical forms as measured by iGC. It is observed that the surface energy of PMMA decreases as the surface coverage increases, although the variations are not large. It is known that the probe gases preferentially adsorb to the higher energy sites first, followed by the lower energy sites of sample surfaces; consequently, the dispersive surface energy obtained by iGC is slightly higher than those values obtained from contact angle measurements.

Next, we expand our demonstration of 2D iGC to include the tunable acid/base character of the polymer coatings. For this, we chose poly(acrylic acid) (PAA) as a model material, since the backbone of the polymer is similar to PMMA, but the side group contains an ionizable carboxylic acid group. We can tune the acid/base character of the carboxyl groups simply by adjusting the pH of the casting solution to be below (pH ≈ 2) or above (pH ≈ 7) the pK_a of the carboxylic acid group (pK_a ≈ 4.5). At pH ≈ 2, the carboxyl groups exist primarily as −COOH (Lewis acid). However, at pH ≈ 7, dissociation of the carboxylic acid occurs, and the carboxyl group exists primarily as the anion −COO$^-$Na$^+$ (Lewis base). Moreover, PAA is a water-soluble polymer that makes traditional water contact angle measurements impossible. Thus, 2D iGC has a distinct advantage, since the concentration of injected probe molecules is within the limit of infinite dilution, eliminating the risk of swelling or dissolution of the polymer thin film or coating. As shown in Figure 2a,b, both the dispersive and acid−base polar surface energies of the PAA coating cast from pH 2 are greater than PAA cast from pH 7 at equivalent surface coverage up to $n/n_m \approx 0.1$. The dispersive surface energy of the PAA cast at pH 2 is in the range of 45.1−50.2 mJ/m^2, and that of the PAA cast at pH 7 is in the range of 40.6−44.0 mJ/m^2. The lower surface energies for the PAA cast at pH 7 are possibly due to the higher resonance hybrid stabilization effect, leading to energetically less active surface and the consequent weaker intermolecular interactions between probe molecules and carboxylate anion groups. In addition, with an increase of pH by adding NaOH, acidic carboxylic groups react with NaOH to form salts (COO$^-$Na$^+$), leading to additional waters of hydration and further decreasing the molecular interactions with probe molecules.[45] Overall, the relative surface basic character (K_b/K_a) is higher for PAA cast from pH 7 when compared to PAA cast from pH 2, indicating more electron-donating Lewis basic sites and fewer Lewis acidic sites (Figure 2c). This can be ascribed to the deprotonation of the carboxyl group and significant increase of electron density upon increasing pH.[46]

Finally, we demonstrate the ability of 2D iGC to measure surface energy and surface energy heterogeneity of a polymer thin film with nanoscale roughness. Here, we chose poly(ethylene oxide) (PEO) as it is a semicrystalline polymer where the crystalline domains alter the surface topography of the thin film, which manifests as nanoscale surface roughness. Accurately measuring the surface energy by surface wetting characterization and more importantly the surface energy heterogeneity of such thin films using contact angle measurements is difficult due to the semicrystalline nature of PEO and

https://doi.org/10.1021/acs.langmuir.4c01400
Langmuir 2024, 40, 14037−14044

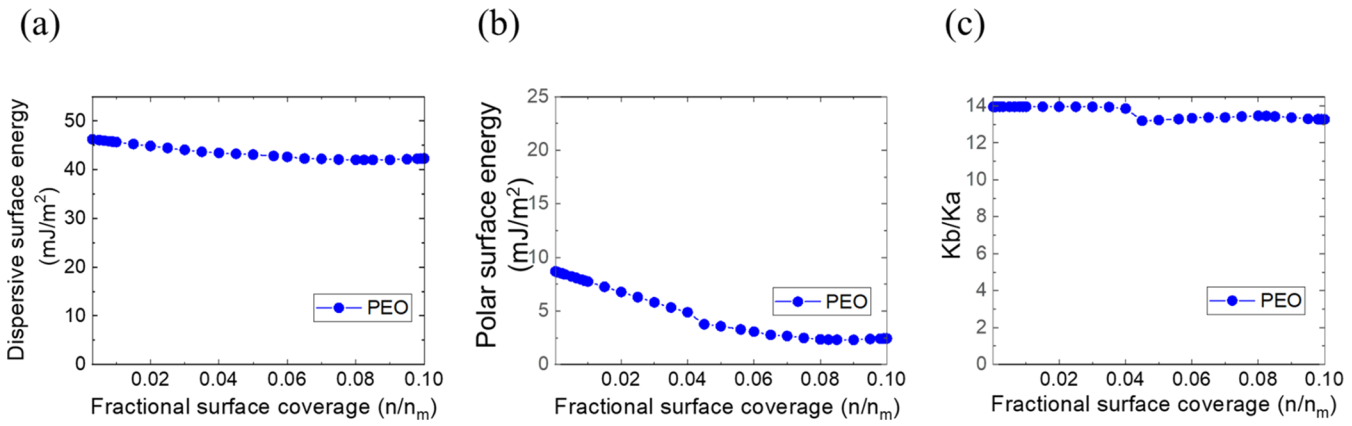

Figure 3. (a) Dispersive and (b) polar (acid−base) surface energy profiles of a poly(ethylene oxide) (PEO) coating. (c) Lewis base parameter/acid parameter ratio (K_b/K_a) profile of the PEO coating as a function of surface coverage (n/n_m).

the resulting nanoscale surface roughness. The advantages of iGC are that surface roughness does not impact the fidelity of the measurement, and iGC can detect heterogeneity in the surface energy as a function of the surface coverage (n/n_m) of the probe molecules. Figure 3a,b shows the surface energy profiles of the PEO coatings at equivalent surface coverage up to $n/n_m \approx 0.1$. Both dispersive and specific (acid−base) surface energies of the PEO coating are smaller than those of the PAA coating cast from pH 2. While the dispersive surface energy of PAA is in the range of 45.1−50.2 mJ/m^2, that of PEO is in the range of 39.6−43.0 mJ/m^2. The acid−base (polar) surface energy of PAA is in the range of 7.0−8.1 mJ/m^2, and that of PEO is in the range of 5.5−6.7 mJ/m^2. It is notable that heterogeneity in the polar surface energy profile of PEO is more pronounced compared to PAA at the surface coverage up to $n/n_m \sim 0.05$. Low surface energy values of PEO compared to the PAA coating can be ascribed to the surface roughness and semicrystalline morphology of the PEO surface, which is consistent with previous studies in that thin-film crystallinity increases as the surface energy decreases.[47] We performed atomic force microscopy (AFM) to compare the surface morphologies and roughness of two coatings (see Figure S5). The surface roughness of PEO films is noticeably higher (11.8 ± 1.8 nm) than that of PAA films (1.3 ± 0.1 nm). The orientation and interaction of probe molecules can be affected by changes in surface roughness, which is possibly associated with an energetically less active surface and lower surface energies of PEO films. In addition, the glass transition temperature of PEO is −50 °C, which suggests that the amorphous regions are in a flexible 'rubbery' state at room temperature. This raises further questions with regard to the spatial distribution of the crystalline structure and structural heterogeneity, which are the topics of future work. As shown in Figure 3c, PEO generally shows lower Lewis acidity and basicity compared to the PAA (pH 2) coating, most likely due to the semicrystalline nature of PEO.

CONCLUSIONS

In summary, we have demonstrated a significant exploration of state-of-the-art iGC that provided versatility in the sample's physical forms from its conventional powder/fiber to embrace supported thin films, with appropriate modification to the iGC injection method and careful sample preparation. We compared the surface energies of PMMA in these different physical sample forms to validate the 2D iGC method. We demonstrated that the surface energy of PMMA thin films deposited on Si wafers measured in the 2D sample holder is in good agreement with the surface energy of PMMA powder or freestanding thin films measured in a conventional column. Surface energy and surface chemistry (Lewis acid−base characteristics) of the PAA coatings with varying ionization of the PAA functional groups and PEO coatings were further investigated. These results revealed that both the dispersive and acid−base polar surface energies of the PAA coating obtained from aqueous solution at pH 2 are greater than those of the PAA coating cast at pH 7. We hypothesize it is due to higher resonance hybrid stabilization of carboxylate anions and the resulting weaker intermolecular interactions with probe molecules at pH 7. 2D iGC was further explored to measure the surface energetics of supported thin films displaying roughness by leveraging the semicrystalline nature of polyethylene oxide (PEO). We demonstrated that both the dispersive and specific (acid−base) surface energies of PEO coatings are smaller than those of the PAA coating cast from pH 2.

The surface roughness and hygroscopic nature of certain thin polymer films can dramatically affect surface wetting characterization by contact angle measurements, whereas topographic features and chemical heterogeneity do not impact the fidelity of iGC measurement. This work provides a tantalizing possibility to our initial endeavor to a 'consilience measurement platform' capable of determining the thermodynamics and transport properties. We envision that this measurement platform will further harness the characterization of various functional coatings, membranes, and surface chemistries. As a promising perspective, we are working on modifications of the clamshell 2D sample holder with precise temperature control for the investigation of solubility parameters of thin films and coatings as well as the introduction of antagonistic gases that will reveal the specific chemical interactions with the coating and the coating's surface properties.

ASSOCIATED CONTENT

Supporting Information

The Supporting Information is available free of charge at https://pubs.acs.org/doi/10.1021/acs.langmuir.4c01400.

Photographs of the clamshell two-dimensional (2D) sample holder for the 2D inverse gas chromatography (iGC) measurements; graphical illustration of determin-

https://doi.org/10.1021/acs.langmuir.4c01400
Langmuir 2024, 40, 14037−14044

ing nonpolar (dispersive) and specific free surface energies obtained from iGC measurement; thickness of the polymer coatings measured by variable angle spectroscopic ellipsometry; polarization modulation infrared reflection absorption spectroscopy (PM-IRRAS) spectra and chemical structure of poly(methyl methacrylate) (PMMA), poly(acrylic acid) (PAA) cast at pH 2, PAA cast at pH 7, and polyethylene oxide (PEO) thin films; nonpolar (dispersive) and polar (acid−base) surface energies of PMMA 21 (M_w: 177 k g mol^{-1}) in different material forms; and height, phase, and 3D height AFM images of PEO thin films, phase and 3D height AFM images of PAA thin films cast at pH 2, and photographs showing the contact angles of methylene iodide and water droplets on PEO thin films (PDF)

AUTHOR INFORMATION

Corresponding Author

Jeremiah W. Woodcock − *Materials Science and Engineering Division, National Institute of Standards and Technology, Gaithersburg, Maryland 20899, United States*; Email: jeremiah.woodcock@nist.gov

Authors

Whirang Cho − *Materials Science and Engineering Division, National Institute of Standards and Technology, Gaithersburg, Maryland 20899, United States; Department of Chemistry, American University, Washington, D.C. 20016, United States*; Present Address: Chemistry Department, United States Naval Academy, Annapolis, Maryland 21402, United States; orcid.org/0000-0002-6708-3336

Lucas Q. Flagg − *Materials Science and Engineering Division, National Institute of Standards and Technology, Gaithersburg, Maryland 20899, United States*; orcid.org/0000-0002-2798-5650

John R. Hoffman − *Materials Science and Engineering Division, National Institute of Standards and Technology, Gaithersburg, Maryland 20899, United States*

Daniel Burnett − *Surface Measurement Systems, Allentown, Pennsylvania 18103, United States*

Anett Kondor − *Surface Measurement Systems, Allentown, Pennsylvania 18103, United States*

Douglas M. Fox − *Materials Science and Engineering Division, National Institute of Standards and Technology, Gaithersburg, Maryland 20899, United States; Department of Chemistry, American University, Washington, D.C. 20016, United States*; orcid.org/0000-0002-0533-2093

Christopher M. Stafford − *Materials Science and Engineering Division, National Institute of Standards and Technology, Gaithersburg, Maryland 20899, United States*; orcid.org/0000-0002-9362-8707

Complete contact information is available at: https://pubs.acs.org/10.1021/acs.langmuir.4c01400

Notes

The authors declare no competing financial interest.

ACKNOWLEDGMENTS

Financial support from Materials Science and Engineering Division (MSED) at the National Institute of Standards and Technology (Grant # 70NANB18H225) is gratefully acknowledged. The authors thank Dr. Chad Snyder, NIST, for useful discussions.

REFERENCES

(1) Strafford, K.; Subramanian, C. Surface engineering: an enabling technology for manufacturing industry. *J. Mater. Process. Technol.* **1995**, *53* (1−2), 393−403.

(2) Strafford, K. N.; Datta, P. K.; Gray, J. S. *Surface Engineering Practice: Processes, Fundamentals, and Applications in Corrosion and Wear*; Ellis Horwood, 1990.

(3) Bao, Z.; Dodabalapur, A.; Lovinger, A. J. Soluble and processable regioregular poly (3-hexylthiophene) for thin film field-effect transistor applications with high mobility. *Appl. Phys. Lett.* **1996**, *69* (26), 4108−4110, DOI: 10.1063/1.117834.

(4) Cho, J. H.; Lee, J.; Xia, Y.; Kim, B.; He, Y.; Renn, M. J.; Lodge, T. P.; Frisbie, C. D. Printable ion-gel gate dielectrics for low-voltage polymer thin-film transistors on plastic. *Nat. Mater.* **2008**, *7* (11), 900−906.

(5) Chang, C.-C.; Pai, C.-L.; Chen, W.-C.; Jenekhe, S. A. Spin coating of conjugated polymers for electronic and optoelectronic applications. *Thin Solid Films* **2005**, *479* (1−2), 254−260.

(6) Kawase, T.; Shimoda, T.; Newsome, C.; Sirringhaus, H.; Friend, R. H. Inkjet printing of polymer thin film transistors. *Thin Solid Films* **2003**, *438-439*, 279−287.

(7) Son, H.; Chau, A. L.; Davis, C. S. Polymer thin film adhesion utilizing the transition from surface wrinkling to delamination. *Soft Matter* **2019**, *15* (31), 6375−6382.

(8) Fowkes, F. M. Attractive forces at interfaces. *Ind. Eng. Chem.* **1964**, *56* (12), 40−52.

(9) Van Oss, C. J.; Good, R.; Chaudhury, M. Additive and nonadditive surface tension components and the interpretation of contact angles. *Langmuir* **1988**, *4* (4), 884−891.

(10) Johnson, K. L.; Kendall, K.; Roberts, A. Surface energy and the contact of elastic solids. *Proc. R. Soc. London, Ser. A* **1971**, *324* (1558), 301−313.

(11) Law, K.-Y.; Zhao, H. *Surface Wetting: Characterization, Contact Angle, and Fundamentals*; Springer, 2016.

(12) Amrei, M.; Davoudi, M.; Chase, G.; Tafreshi, H. V. Effects of roughness on droplet apparent contact angles on a fiber. *Sep. Purif. Technol.* **2017**, *180*, 107−113.

(13) Woodward, J. T.; Gwin, H.; Schwartz, D. Contact angles on surfaces with mesoscopic chemical heterogeneity. *Langmuir* **2000**, *16* (6), 2957−2961.

(14) Chau, T. A review of techniques for measurement of contact angles and their applicability on mineral surfaces. *Miner. Eng.* **2009**, *22* (3), 213−219.

(15) Yuan, Y.; Lee, T. R. Contact angle and wetting properties. In *Surface Science Techniques*; Springer, 2013; pp 3−34.

(16) Sedev, R.; Petrov, J.; Neumann, A. Effect of Swelling of a Polymer Surface on Advancing and Receding Contact Angles. *J. Colloid Interface Sci.* **1996**, *180* (1), 36−42.

(17) Mohammadi-Jam, S.; Waters, K. Inverse gas chromatography applications: A review. *Adv. Colloid Interface Sci.* **2014**, *212*, 21−44.

(18) Yampolskii, Y.; Belov, N. Investigation of polymers by inverse gas chromatography. *Macromolecules* **2015**, *48* (19), 6751−6767.

(19) Voelkel, A.; Strzemiecka, B.; Adamska, K.; Milczewska, K. Inverse gas chromatography as a source of physiochemical data. *J. Chromatogr. A* **2009**, *1216* (10), 1551−1566.

(20) Tisserand, C.; Calvet, R.; Patry, S.; Galet, L.; Dodds, J. A. Comparison of Two Techniques for the Surface Analysis of Alumina (Al2O3): Inverse Gas Chromatography at Finite Concentration (IGC-FC) and Dynamic Vapor Sorption (DVS). *Powder Technol.* **2009**, *190* (1−2), 53−58.

(21) Thielmann, F. Introduction into the Characterisation of Porous Materials by Inverse Gas Chromatography. *J. Chromatogr. A* **2004**, *1037* (1−2), 115−123.

(22) Zhou, Q.; Cadwallader, K. R. Inverse Gas Chromatographic Method for Measurement of Interactions between Soy Protein Isolate

and Selected Flavor Compounds under Controlled Relative Humidity. *J. Agric. Food Chem.* **2004**, *52* (20), 6271−6277.
(23) Menzel, R.; Lee, A.; Bismarck, A.; Shaffer, M. S. Inverse Gas Chromatography of As-Received and Modified Carbon Nanotubes. *Langmuir* **2009**, *25* (14), 8340−8348.
(24) Heng, J. Y. Y.; Pearse, D. F.; Thielmann, F.; Lampke, T.; Bismarck, A. Methods to Determine Surface Energies of Natural Fibres: A Review. *Compos. Interfaces* **2007**, *14* (7−9), 581−604.
(25) Grimsey, I. M.; Feeley, J. C.; York, P. Analysis of the Surface Energy of Pharmaceutical Powders by Inverse Gas Chromatography. *J. Pharm. Sci.* **2002**, *91* (2), 571−583.
(26) Ferguson, A.; Caffrey, I. T.; Backes, C.; Coleman, J. N.; Bergin, S. D. Differentiating Defect and Basal Plane Contributions to the Surface Energy of Graphite using Inverse Gas Chromatography. *Chem. Mater.* **2016**, *28* (17), 6355−6366.
(27) Bayati, F.; Boluk, Y.; Choi, P. Inverse gas chromatography study of the permeability of aroma through hydroxypropyl xylan films. *ACS Sustainable Chem. Eng.* **2015**, *3* (12), 3114−3122.
(28) Klein, G. L.; Pierre, G.; Bellon-Fontaine, M.-N.; Graber, M. Inverse gas chromatography with film cell unit: An attractive alternative method to characterize surface properties of thin films. *J. Chromatogr. Sci.* **2015**, *53* (8), 1233−1238.
(29) Flagg, L. Q.; Cho, W.; Woodcock, J.; Li, R.; Ro, H. W.; Delongchamp, D. M.; Richter, L. J. Improved Organic Electrochemical Transistors via Directed Crystallizable Small Molecule Templating. *Chem. Mater.* **2024**, *36*, 1352−1361, DOI: 10.1021/acs.chemmater.3c02489.
(30) Hoffman, J. R.; Baumann, A. E.; Stafford, C. M. Thickness dependent CO2 adsorption of poly(ethyleneimine) thin films for direct air capture. *Chem. Eng. J.* **2024**, *481*, No. 148381.
(31) Ho, R.; Heng, J. Y. A review of inverse gas chromatography and its development as a tool to characterize anisotropic surface properties of pharmaceutical solids. *KONA Powder Part. J.* **2013**, *30*, 164−180.
(32) Cordeiro, N.; Gouveia, C.; Moraes, A.; Amico, S. Natural fibers characterization by inverse gas chromatography. *Carbohydr. Polym.* **2011**, *84* (1), 110−117.
(33) Schultz, Ja.; Lavielle, L.; Martin, C. The role of the interface in carbon fibre-epoxy composites. *J. Adhes.* **1987**, *23* (1), 45−60.
(34) Das, S. C.; Larson, I.; Morton, D. A.; Stewart, P. J. Determination of the polar and total surface energy distributions of particulates by inverse gas chromatography. *Langmuir* **2011**, *27* (2), 521−523.
(35) Van Oss, C. J.; Chaudhury, M. K.; Good, R. J. Interfacial Lifshitz-van der Waals and polar interactions in macroscopic systems. *Chem. Rev.* **1988**, *88* (6), 927−941.
(36) Ozcan, C.; Hasirci, N. Evaluation of surface free energy for PMMA films. *J. Appl. Polym. Sci.* **2008**, *108* (1), 438−446.
(37) Surface Energy Data for PMMA: Poly(methylmethacrylate), CAS # 9011−14−7, 2009 https://www.accudynetest.com/polymer_surface_data/pmma_polymethylmethacrylate.pdf (accessed Jan 30, 2024).
(38) Khodakarami, M.; Alagha, L.; Burnett, D. J. Probing surface characteristics of rare earth minerals using contact angle measurements, atomic force microscopy, and inverse gas chromatography. *ACS Omega* **2019**, *4* (8), 13319−13329.
(39) Andrzejewska, E.; Voelkel, A.; Andrzejewski, M.; Maga, R. Examination of surfaces of solid polymers by inverse gas chromatography: 2. Acid-base properties. *Polymer* **1996**, *37* (19), 4333−4344.
(40) Voelkel, A. Inverse gas chromatography: characterization of polymers, fibers, modified silicas, and surfactants. *Crit. Rev. Anal. Chem.* **1991**, *22* (5), 411−439.
(41) Meyer, R.; Mueller, K.; Naumov, S.; Bauer, F.; Enke, D. Characterization of polar surface groups on siliceous materials by inverse gas chromatography and the enthalpy−entropy compensation effect. *Front. Chem.* **2023**, *11*, No. 1084046.
(42) Shi, B.; Zhang, Q.; Jia, L.; Liu, Y.; Li, B. Surface Lewis acid−base properties of polymers measured by inverse gas chromatography. *J. Chromatogr. A* **2007**, *1149* (2), 390−393.
(43) Sreekanth, T.; Basivi, P. K.; Nagajyothi, P.; Dillip, G.; Shim, J.; Ko, T.; Yoo, K. Determination of surface properties and Gutmann's Lewis acidity−basicity parameters of thiourea and melamine polymerized graphitic carbon nitride sheets by inverse gas chromatography. *J. Chromatogr. A* **2018**, *1580*, 134−141.
(44) van Asten, A.; van Veenendaal, N.; Koster, S. Surface characterization of industrial fibers with inverse gas chromatography. *J. Chromatogr. A* **2000**, *888* (1−2), 175−196.
(45) Dubas, S. T.; Schlenoff, J. B. Swelling and smoothing of polyelectrolyte multilayers by salt. *Langmuir* **2001**, *17* (25), 7725−7727.
(46) Carboxylic Acids, LibreTexts Chemistry. https://chem.libretexts.org/Bookshelves/Organic_Chemistry/Book%3A_Organic_Chemistry_A_Carbonyl_Early_Approach_(McMichael)/01%3A_Chapters/1.12%3A_Carboxylic_Acids (accessed 01/09/2024).
(47) Zhang, F.; Mohammadi, E.; Luo, X.; Strzalka, J.; Mei, J.; Diao, Y. Critical role of surface energy in guiding crystallization of solution-coated conjugated polymer thin films. *Langmuir* **2018**, *34* (3), 1109−1122.

https://doi.org/10.1021/acs.langmuir.4c01400
Langmuir 2024, 40, 14037−14044